

## Preparation and Study of SnO<sub>2</sub> MOM Structure by The Thermal Vacuum Evaporation Deposition

Dr. Luqman Sufer Ali  
luqmansufer@yahoo.com

Omar Ghanim Ghazal  
omar.unom@yahoo.com

Electrical Engineering Dept. / College of Engineering

### Abstract

Resistive switching random access memory is one of the novel nonvolatile memory technologies that, has a promising future for replacing the conventional FLASH memory. In this work a detailed study made about the types of operations and understanding the mechanisms of the resistance changing in the device. SnO<sub>2</sub> thin films are deposited by using Thermal Vacuum Evaporation deposition method at room temperature on Al/glass substrate to produce Al/SnO<sub>2</sub>/Al/glass device structure. Optical properties are taken to measure the optical band gap of SnO<sub>2</sub>. Resistive switching is observed by taking current voltage readings at room temperature. RRAM cell showed unipolar resistive switching behavior with no overlapping between reset and set voltage (1.5V, 2.5V respectively), also between high and low resistance states (7.7K $\Omega$ , 106 $\Omega$ ). Good retention and endurance are obtained and the ratio between HRS to LRS has been found to be at least (41) within 21 cycles.

**Keywords:** RRAM, Resistive Switching, nonvolatile memory, SnO<sub>2</sub> thin film.

### باستخدام ترسيب التفريغ الحراري SnO<sub>2</sub> - MOM تحضير ودراسة التركيب

عمر غانم غزال

أ.م.د. لقمان سفر علي

كلية الهندسة / قسم الهندسة الكهربائية

### الخلاصة

الذاكرة العشوائية المعتمدة على التغير في المقاومة هي إحدى التقنيات الحديثة للذاكرة غير المتطايرة ولها مستقبل واعد في قدرتها على استبدال الذاكرة الحالية المستخدمة نوع فلاش. في هذا البحث تمت الدراسة بشكل مفصل لأنواع هذه الذاكرة حسب طريقة عملها وكذلك آلية الخلية والتغير الذي يطرأ عليها عند تغير قيمة مقاومتها. تم ترسيب SnO<sub>2</sub> بطريقة التبخير الحراري في درجة حرارة الغرفة وعلى سطح مكون من Al/glass وكذلك الطبقة العليا كانت المنيوم. وقد اخذت قياسات الخصائص الضوئية لسطح SnO<sub>2</sub> لقياس فجوة الطاقة. التغير في المقاومة تم ملاحظته عند اخذ قياسات التيار مع الفولتية في درجة حرارة الغرفة. وقد اظهرت خلية الذاكرة تغير في المقاومة نوع احادي الفولتية مع عدم وجود تداخل بين فولتيات العمل (reset, set) بما يقارب (1.5V, 2.5V) كذلك كانت قيمة المقاومة العليا والدنيا (7.7 K $\Omega$ , 106 $\Omega$ ). وقد اظهرت هذه الذاكرة المصنع تكراراً بحدود (21) دورة وديمومة للمعلومة مع نسبة للمقاومة العليا الى والمقاومة الدنيا وبأسوء الظروف بحدود (41).

Received: 24 - 4 - 2012

Accepted: 18 - 4 - 2013

## 1- Introduction:-

Modern electronic devices are continual to demand smaller, faster, and denser semiconductor, nonvolatile memories[1,2]. The conventional flash memory has scaled down to achieve large capacity and reduce the access time [1,2,3].

However scaling the conventional memories is approaching the technical and physical limits and the growth industry, in productivity, is needed to be continual [1,2]. For decreasing the size of electronic devices and the desire to reduce the access time in terms of speed, endurance, and retention properties novel materials, and fabrication techniques must be introduced. As a result will help to produce new electrical devices to meet the demands of the electronic industry growth in the future [3,4,5].

Simultaneously a novel storage methods called "Universal Memory"[6], has attracted more attention to some of the recently ideas. These techniques may include silicon oxide nitride silicon memory (SONOS), magneto resistive random access memory (MRAM), ferroelectric random access memory (FeRAM), conducting bridge random access memory (CBRAM), phase change random access memory (PRAM), and resistive random access memory (RRAM) [2,4,5,6,7].

## 2- Resistive Random Access Memory(RRAM):-

Resistive Random Access Memory is, generally denoting the memory technology that depends upon the resistance change to store the information [6]. This technology is based on new materials, such as transition metal oxides, and organic compounds which show a resistive switching (changing) phenomenon [2].

Recently, this kind of the novel technology of nonvolatile memory, has attracted great attention due to its potential for the replacement of flash memory in the next generation nonvolatile memory (NVM) application[1,3,8]. The main motivation, behind good expectations about the widely use of this type of memory in the near future, is that the RRAM cell has a simple structure (Fig.1(a)) of two metal electrodes separated by an insulating or semiconductor materials like a two terminals capacitor structure [1,2].

This structure makes it easier in integration with current complementary metal oxide semiconductor technology (CMOS) and a highly scalable cross point structure as shown in (Fig.1(b)), where a bistable material is sandwiched between the parallel bottom electrodes and the orthogonal top electrodes, has been proposed because the memory cell size can be reduced to an area of  $4F^2$  ( $F$  = minimize feature size on a given process). This enable us to fabricate a high density memory, and potentially even smaller if the memory cells are stacked in three dimensions[1,2]. The resistive switching phenomenon was observed in varies materials such as transition metal oxides (NiO, TiO<sub>2</sub>, HfO<sub>2</sub>, ZnO, and Al<sub>2</sub>O<sub>3</sub>), perovskite oxides (SrZrO<sub>3</sub>), chalcogenide materials (GeSbTe), ferroelectric (PbZr<sub>0.52</sub>Ti<sub>0.48</sub>O<sub>3</sub>), and ferromagnetic (MgO)[1,2,8].

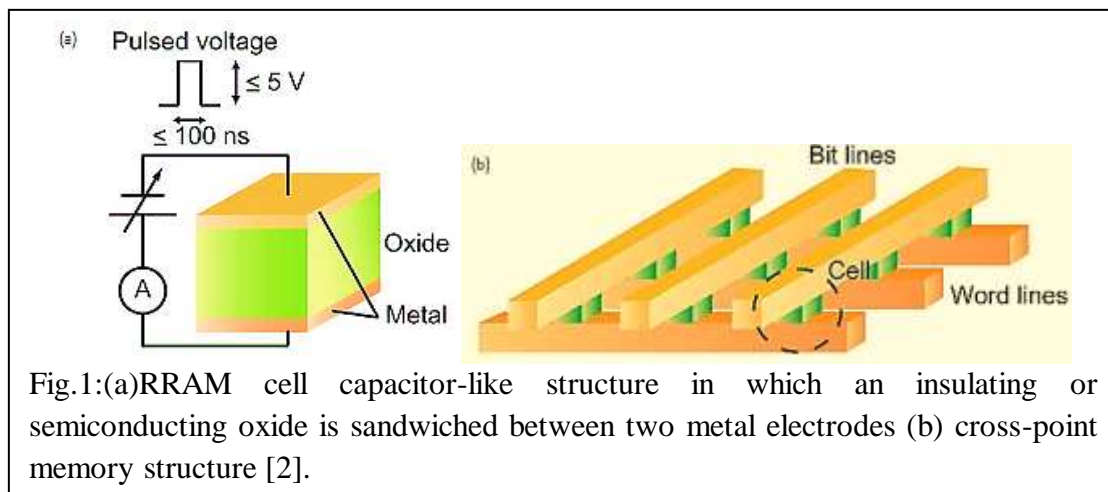


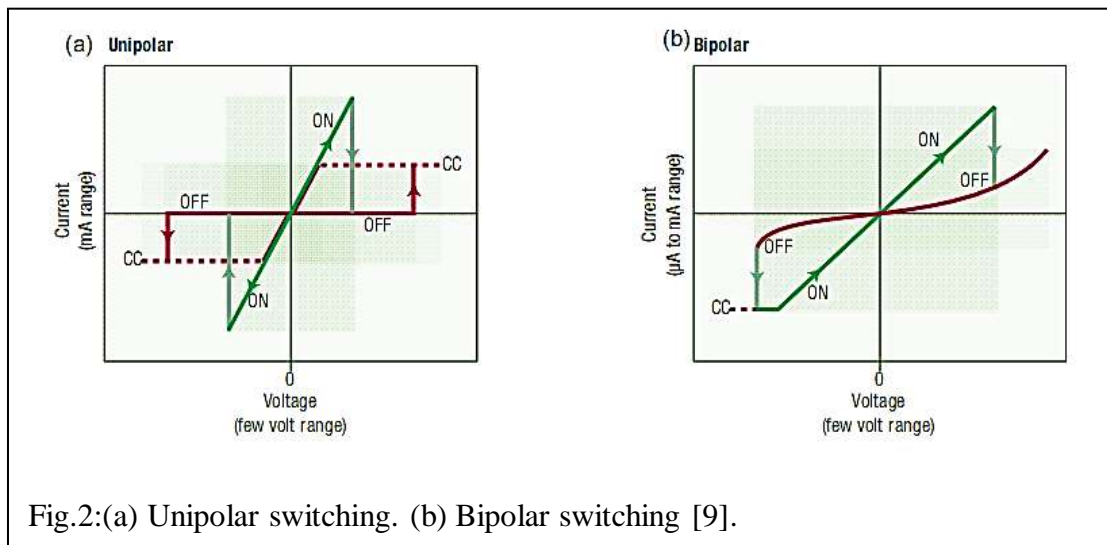
Fig.1:(a)RRAM cell capacitor-like structure in which an insulating or semiconducting oxide is sandwiched between two metal electrodes (b) cross-point memory structure [2].

### 3- RRAM Operation Techniques:-

A unipolar, and bipolar switching are the only two conventional operation proposed. In unipolar operation, executes the programming and erasing by using short and long pulse, or by using high and low voltage with the same voltage polarity [6].

A prepared memory cell (before the formation) is in a highly resistive state and is put into a low resistance state (LRS) by applying a high voltage stress, this is called the "Forming Process". The cell is switched back to a high resistive state (HRS) when applying a threshold voltage called "Reset Process". Switching from HRS to a LRS is called "Set Process". This is achieved by applying a threshold voltage that is larger than the reset voltage (Fig.2(a))[2].

In Bipolar type the switching is achieved by short pulses with opposite voltage polarity (depending on the polarity) and in some systems, no CC is used (Fig.2(b)) [2].



### 4- Mechanism of Operation:-

Two types of resistive switching mechanisms are used to describe the formation, reset, and set operations at RRAM devices: filamentary conducting path and interface-type conducting path [2]:

#### 4.1- Filamentary Conducting Path:-

It has three stages, the first is the forming process happens at start of using the device where conducting paths form as a soft breakdown in the dielectric material. The second process after the forming is the reset process in which a rupture of filaments takes place during the applying of the reset voltage. The last stage is the filament formation during the set process when the set voltage is applied (Fig.3(a)) [2]. The device can be switched between HRS and LRS a large number of times. Thermal redox (oxidation and reduction) and/or anodization near the interface between the metal electrode and the oxide is widely considered to be the mechanism behind the formation and rupture of the filaments. In contrast, in bipolar-type switching, electrochemical migration of oxygen ions is regarded as the driving mechanism [2].

#### 4.2- Interface-Type Conducting Path:-

As shown in (Fig.3(b)) this type of mechanism the resistive switching occurs at the interface between metal electrode and the oxide[2]. This switching mechanism is usually related to the bipolar-type resistive switching behavior observed in semiconducting perovskite oxides. In semiconducting oxides a schottky barrier is suggested to be the origin of the contact resistance [2].

The difference between the filament and interface types of resistive switching can be understood by considering the area dependence of the cell resistance. The resistive switching in the interface-type takes place over the whole area of the cell, i.e. the entire interface, whereas switching occurs locally in the filamentary type cell through the formation of filamentary conducting paths [2]. In the schottky model the magnitude of the contact resistance is due to the potential of the barrier or the depletion layer. The depletion layer width depends on the carrier concentration and in this case the oxygen vacancies ,this is thinner for LRS and wider for HRS [2].

#### 5- Tin Oxide (SnO<sub>2</sub>):-

Tin Oxide (SnO<sub>2</sub>) is an abundant material and n-type semiconductor with oxygen vacancies [10].SnO<sub>2</sub> seems to be a good candidate for the solar cell application because of its wide band gap of (3.5-3.6) eV at room temperature [10,11,12,13]. It has also been employed in a wide range of application including solid state gas sensors, liquid crystal displays, transparent conducting electrodes, infrared reflectors, plasma display panels (PDPs), transistors etc.. [11,12]. Although SnO<sub>2</sub> demonstrates orders of magnitude in resistivity change depending on its oxygen vacancies concentration [10], but it has not received much attention for resistive switching application except in recent years as in [10] SnO<sub>2</sub> used with Pt top, Pt/Ti bottom electrodes and also in [14] Ag top, Ti bottom electrodes.

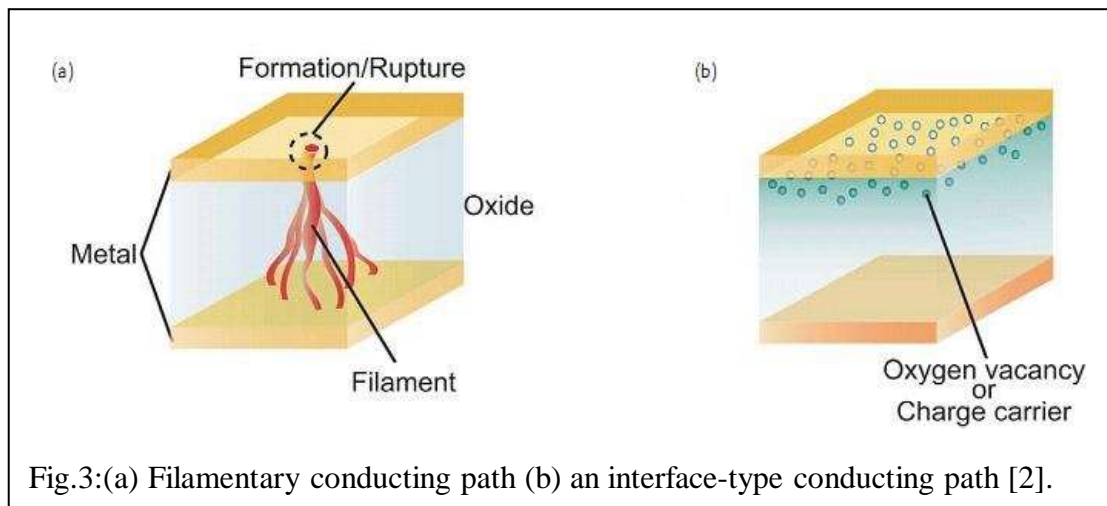


Fig.3:(a) Filamentary conducting path (b) an interface-type conducting path [2].

#### 6- Experimental Details:-

Glass slides with (75 × 25) mm<sup>2</sup> area are used as a substrate, but after passing in a cleaning sequence the same sequence is used for cleaning the prepared masks of ten minutes of immersing in acetone, ten minutes of immersing in distilled water at 150 °C in the oven, washing in a distilled water at room temperature, and finally drying with a hot air beam. The thermal vacuum evaporation deposition by Balzer BA510 coating system is used at room

temperature to carry out the following sorted order of deposits as shown in (Fig.4). Table (1) display the deposited materials, thickness, and the atmosphere properties of deposition operation.

Material	Thickness	Pressure	Rate	Density	Used Boat
Al (Top electrode)	2000 Å	$6 \times 10^{-6}$ mbar	5 Å/sec	2.7 g/cm <sup>3</sup>	Tungsten
SnO <sub>2</sub>	500 Å	$5 \times 10^{-6}$ mbar	1 Å/sec	6.9 g/cm <sup>3</sup>	Molybdenum
Al (Bottom electrode)	2000 Å	$4 \times 10^{-6}$ mbar	5 Å/sec	2.7 g/cm <sup>3</sup>	Tungsten

The used SnO<sub>2</sub> in the deposition was with high purity (99.99%) powder. The region of Aluminum bottom electrode was over all the substrate then putting the first mask (20×25) mm<sup>2</sup> for Tin Oxide layer, and finally the last mask has holes of (6 mm Diameter) in order to deposit the last layer Aluminum top electrode.

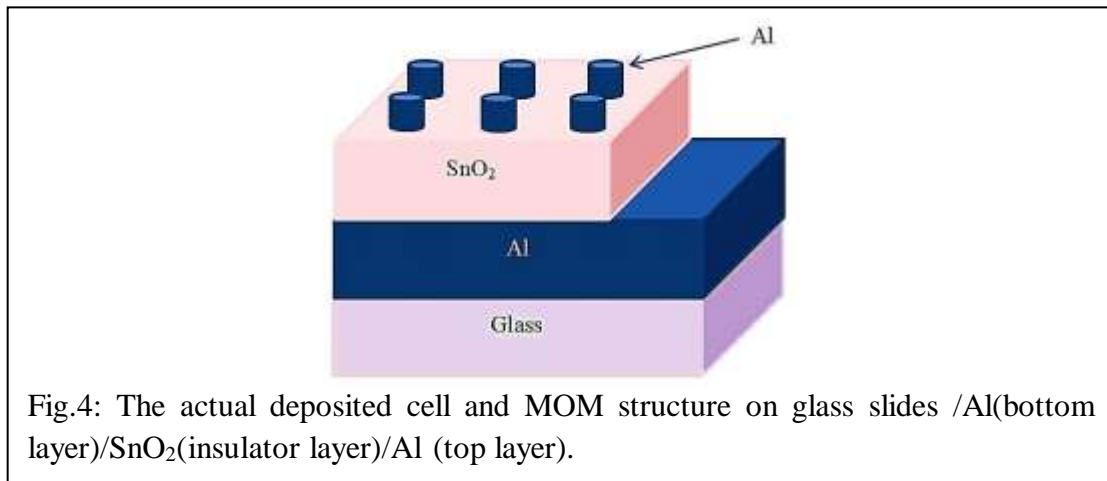


Fig.4: The actual deposited cell and MOM structure on glass slides /Al(bottom layer)/SnO<sub>2</sub>(insulator layer)/Al (top layer).

The Shimadzu UV-1800 Spectrophotometer is used for measuring the optical characteristics of Tin Oxide, VICTOR 86B Digital Multimeter, Keithley 595 Quasistatic C-V Meter, D.C power supply, and DT 9205 Digital Multimeter were used for measuring the current voltage properties.

## 7- Results and Discussion:-

### 7.1- Optical Properties of SnO<sub>2</sub>:

The optical analysis, of SnO<sub>2</sub> thin film samples, is obtained by a UV-1800 Spectrophotometer in the wavelength range of 300nm to 1000nm to measure the transmittance and absorption at room temperature, calculating absorption coefficients and the band gap. The samples are deposited at room temperature, but with different deposition sessions and not at one deposition operation. Fig.5 and Fig.6 presents plot of transmittance and absorption as a function of wavelength respectively for three samples. Optical transitions show that SnO<sub>2</sub> is a direct band gap material [11].

The relation between absorption coefficient ( $\alpha$ ) and the incident photon energy ( $h\nu$ ) for allowed direct transitions is given by [11,15]:

$$\alpha h\nu = A(h\nu - E_g)^{1/2} \quad \dots \dots (1)$$

Where  $\alpha$  is the absorption coefficient, A is a constant, h is Planck's constant ( $6.626 \times 10^{-34}$

Joules sec),  $\nu$  is the frequency, and  $E_g$  is the band gap energy of the material. The absorption coefficient  $\alpha$  is obtained from Lambert's Law that describes the relationship between transmission, absorption and thickness [16,17]:

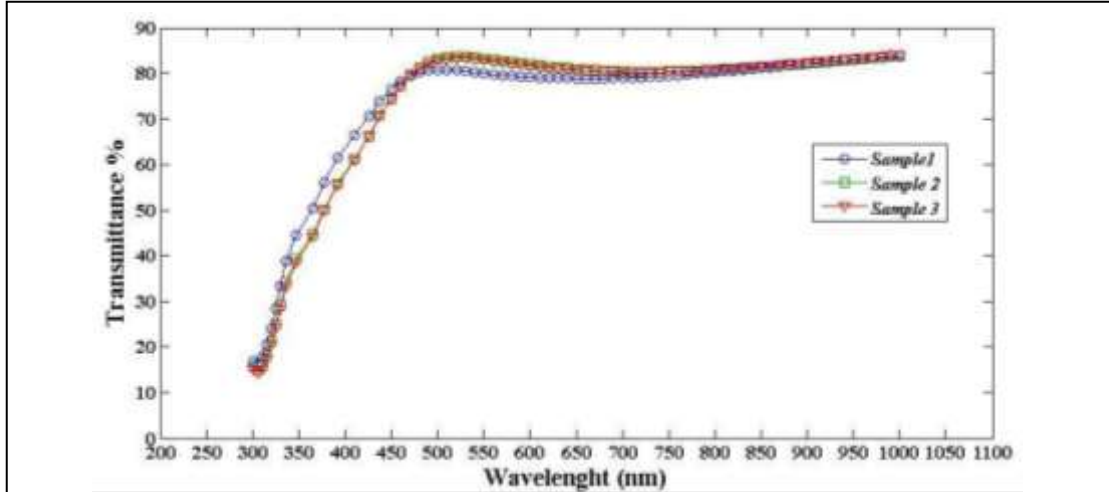


Fig.5: Optical transmittance of SnO<sub>2</sub> thin film for three deposited samples of thickness 40 nm at room temperature.

$$T = e^{-\alpha t} \quad \dots \dots (2)$$

Or rewritten as

$$\alpha = -\frac{1}{t} \ln T \quad \dots \dots (3)$$

Where  $t$  is the thickness of the measured samples, and  $T$  is the Transmittance. A plot of  $(\alpha h\nu)^2$  versus photon energy ( $h\nu$ ) as shown in (Fig.7) was used to obtain the value of the direct band gap by extrapolating the linear portion of the curves to zero absorption [11,12,13,16].

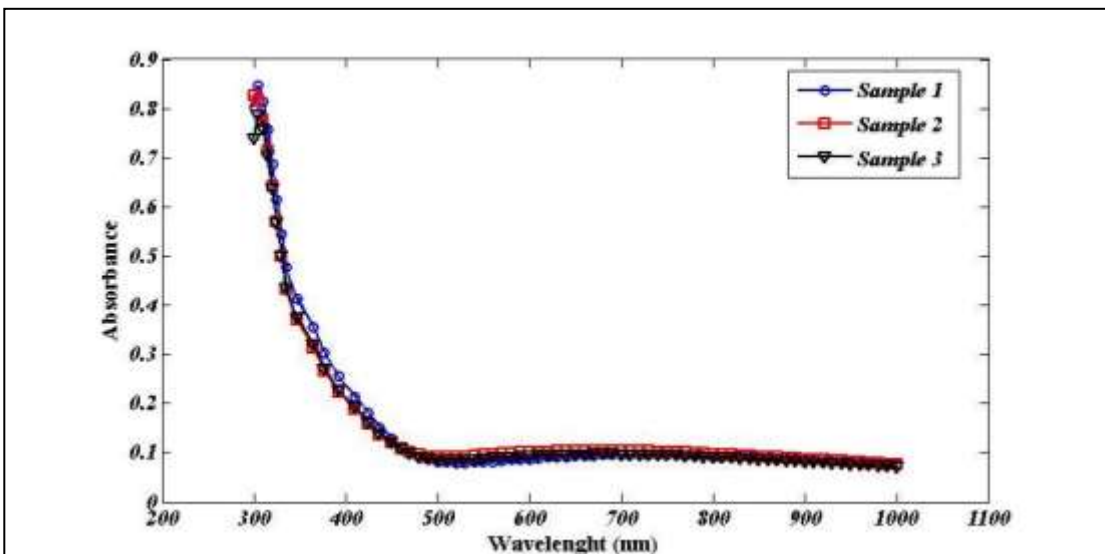


Fig.6: Optical absorbance of SnO<sub>2</sub> thin film for three as deposited samples of thickness 40 nm at room temperature.

As presented in (Fig.7) the value of the optical band gap of deposited SnO<sub>2</sub> thin film is 3.62 eV for the first sample and 3.6 eV for the second and third sample the average band gap is 3.606 eV and almost in agreement with the reported values of band gaps data in [11,12,13].

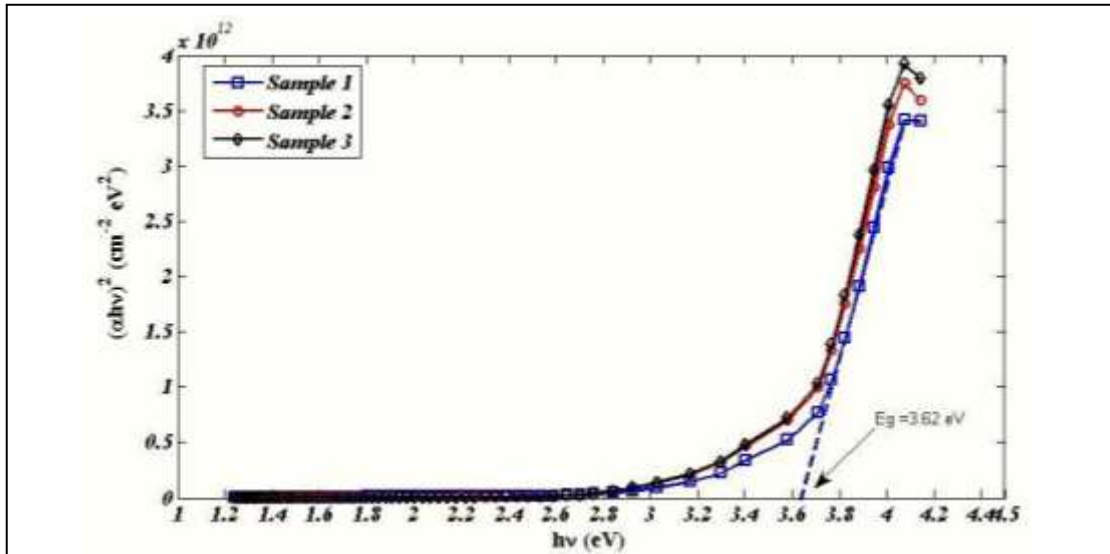


Fig.7: Plot of  $(\alpha hv)^2$  vs. photon energy( $h\nu$ ) of SnO<sub>2</sub> thin films with extrapolating straight line portion to evaluate the optical band gap of SnO<sub>2</sub> .

## 7.2- Current – Voltage Characteristics:

All the I-V measurements are taken at room temperature. The measuring circuit is shown in Fig.(8) where R1 is potentiometer, R2 variable resistor for the protection of under test sample, V1 and V2 are voltmeters, A is the sample current ammeter , and MOM is the cell. (Fig.9) shows the current-voltage characteristics of MOM memory cell (RRAM cell) based on Al/SnO<sub>2</sub>/Al capacitor.

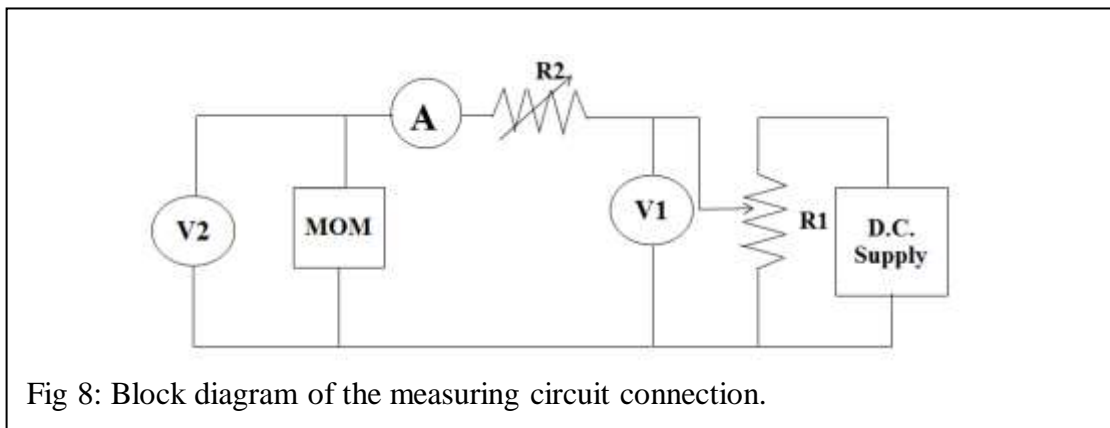


Fig 8: Block diagram of the measuring circuit connection.

Table (2) shows the reading of ammeter A current and the voltage of voltmeter V2 . The deposited thin film was found to behave as a high resistance state of ( $\approx 3.5 \text{ M}\Omega$ ) measured when (0.7 V) applied and reading of current was  $0.2\mu\text{A}$ . The resistive switching phenomenon was not observed in fresh samples, until applying D.C. bias voltage with current compliance of 3.8mA and this procedure, known as the forming process, is necessary to

initiate the switching property of the RRAM cell and is very clear in Fig.10 when drawing the log-linear relationship between the current and voltage.

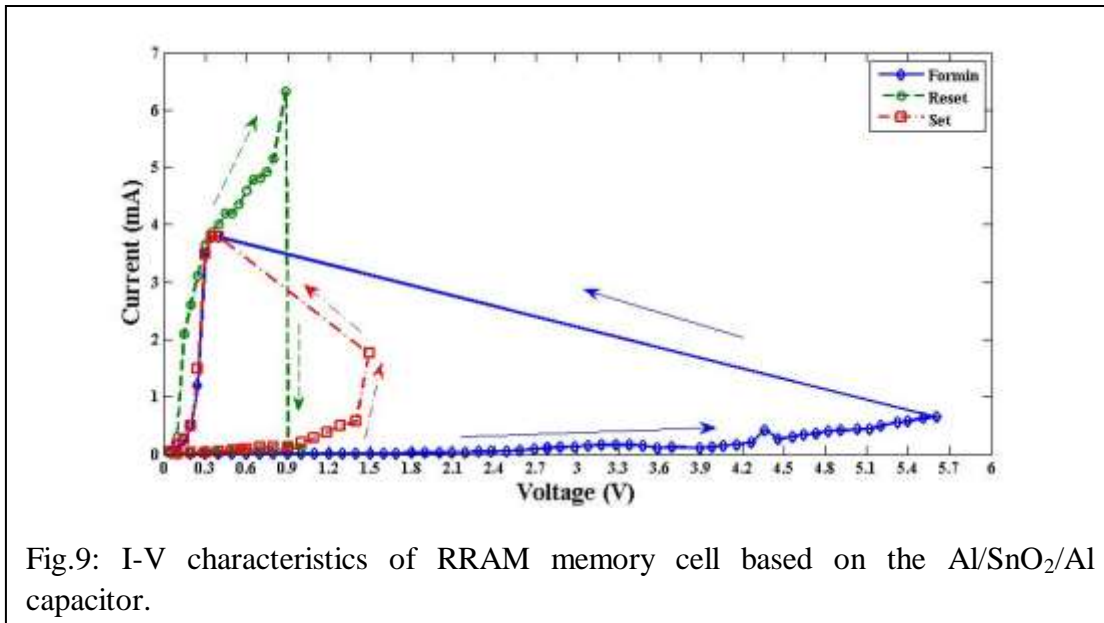


Fig.9: I-V characteristics of RRAM memory cell based on the Al/SnO<sub>2</sub>/Al capacitor.

The forming voltage in this work is about 5.62V. The forming process was made twice before observing the resistive switching. This forming voltage for SnO<sub>2</sub> in this work is higher than the reported in reference [14] (4-5 volt) for other metals used with tin oxide, because of the larger area of the top electrode used in this work.

As a result of the forming process the devices switched to low resistance state (LRS) i.e the resistance became (105 Ω) with a drop voltage of (0.4 V), this resistance stay at its low value until increasing the applied voltage to a value of range (0.68 – 1.5 V) called Reset voltage with the same polarity a sudden drop of current is achieved and the resistance of the cell is switched to high resistance state (HRS) the current dropped to about (127-150 μA) (see table 3). Hence the nonvolatile memory OFF state is done. While increasing the voltage with same polarity a going up of current appears at higher voltage than reset voltage of (1.13 – 2.5 V) called Set Voltage converts the cell to a LRS (table 4). Hence the nonvolatile memory ON state is achieved. (Fig.11) shows the resistance changing gradually with applying voltages for both reset and set. Comparing with other work such as that in [7] ( 1.2-2V) this is a higher set voltage.

The set switching from HRS to LRS must sweep with a current compliance to protect the sample from a permanent breakdown. Note that the reset process requires higher current than the limited current for reset process (CC). Changing the polarity of the voltage to negative shows a symmetrical behavior.

A small spreading in the value of reset and set voltages was appeared, but with no overlapped window of switching voltages between the two resistance states, which are important for nonvolatile memory application [6].



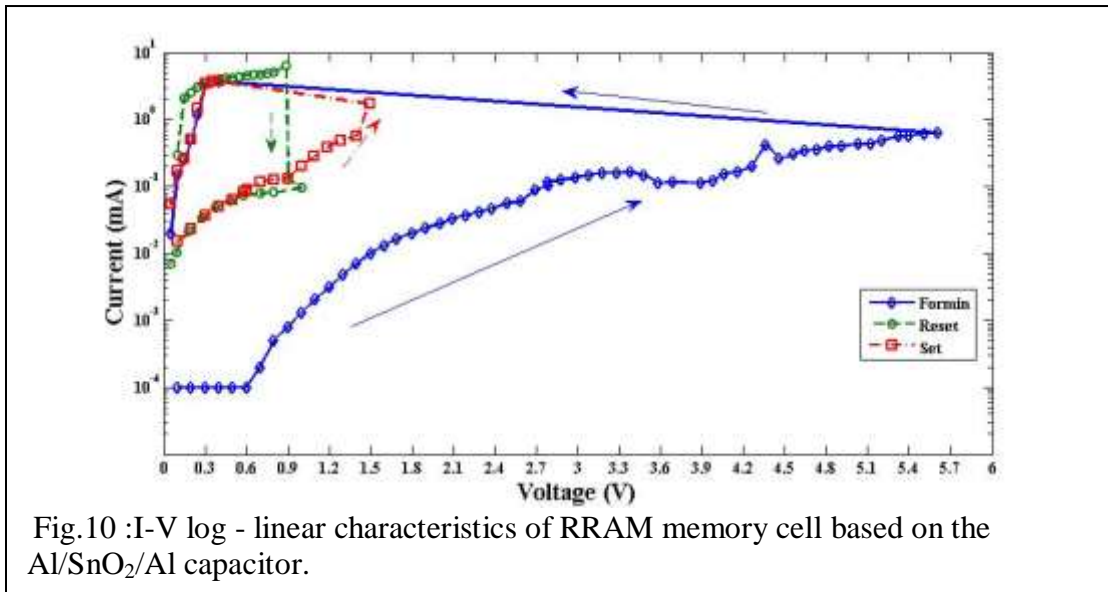


Fig.10 :I-V log - linear characteristics of RRAM memory cell based on the Al/SnO<sub>2</sub>/Al capacitor.

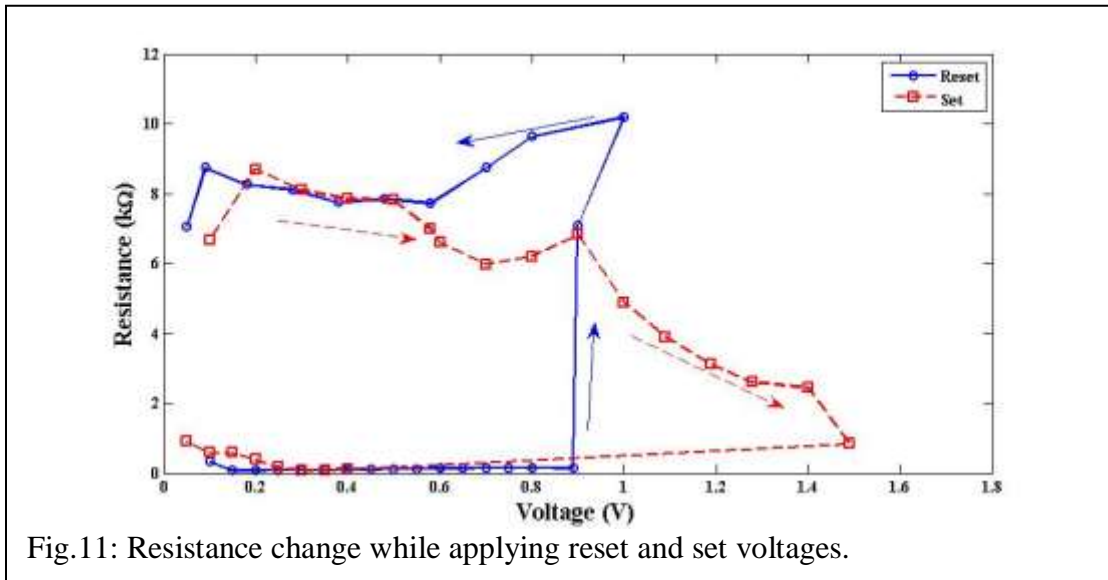


Fig.11: Resistance change while applying reset and set voltages.

The endurance is shown in (Fig.12) by plotting the resistance versus switching cycles for 21 cycles, the resistance was measured at 0.3 V for HRS and LRS at each D.C. sweep. 40.9% max fluctuation was observed in the values of HRS, and a decreasing after 20 cycle, although the devices indicated that more switching is possible at least resistance ratio of 40 order. A retention was performed in order to analyze the devices ability to maintain either the low or high resistance state over time. The retention data over at least 1800 S was taken the HRS showed a good stability with a regularly increasing in the value of LRS, due to oxidation in atmospheric conditions. The HRS is widely distributed in a range of (4.3 - 7.7)KΩ, while the LRS is narrowly distributed in range (106 - 82)Ω. The ratio of HRS to LRS is about (41-94) order within the 21 cycles.

Table 2: Forming Current Voltage Readings

Ameter Reading (A) $\mu$ A	V2 (volt)	R k $\Omega$ (V2/A)
0.1	0.1	1000.000
0.1	0.2	2000.000
0.1	0.3	3000.000
0.1	0.4	4000.000
0.1	0.5	5000.000
0.1	0.6	6000.000
0.2	0.7	3500.000
0.5	0.8	1600.000
0.8	0.9	1125.000
1.3	1	769.231
2.1	1.1	523.810
3.1	1.2	387.097
4.9	1.3	265.306
7	1.4	200.000
10	1.5	150.000
13.2	1.6	121.212
16.6	1.69	101.807
20.2	1.8	89.109
24	1.9	79.167
28	2	71.429
33	2.09	63.333
37.4	2.19	58.556
42	2.29	54.524
47.4	2.38	50.211
56	2.49	44.464
60	2.59	43.167
89	2.69	30.225
105	2.79	26.571
115.5	2.78	24.069
125	2.88	23.040
136	2.98	21.912
150	3.08	20.533
160	3.18	19.875
162	3.28	20.247
165	3.38	20.485
150	3.48	23.200
113	3.58	31.681
117	3.69	31.538
115	3.89	33.826
122	3.98	32.623
154	4.06	26.364
168	4.16	24.762
200	4.26	21.300
420	4.36	10.381
260	4.46	17.154
305	4.56	14.951
350	4.64	13.257
359	4.73	13.175
401	4.82	12.020
410	4.91	11.976
429	5.03	11.725
441	5.12	11.610
490	5.2	10.612
560	5.32	9.500
573	5.4	9.424
625	5.51	8.816
648	5.61	8.657
3800	0.4	0.105
3800	0.35	0.092
3500	0.3	0.086
1200	0.25	0.208
500	0.2	0.400
250	0.15	0.600
150	0.1	0.667
20	0.05	2.500

Table 3: Reset Current Voltage Readings

Ameter Reading (A) $\mu$ A	V2 (volt)	R k $\Omega$ (V2/A)
300	0.1	0.333
2100	0.15	0.071
2600	0.2	0.077
3109	0.25	0.080
3650	0.3	0.082
3870	0.35	0.090
4000	0.4	0.100
4200	0.45	0.107
4210	0.5	0.119
4350	0.55	0.126
4600	0.6	0.130
4780	0.65	0.136
4810	0.7	0.146
4930	0.75	0.152
5150	0.8	0.155
6320	0.89	0.141
127	0.9	7.087
98	1	10.204
83	0.8	9.639
80	0.7	8.750
75	0.58	7.733
61	0.48	7.869
49	0.38	7.755
34.5	0.28	8.116
21.8	0.18	8.257
10.3	0.09	8.738
7.1	0.05	7.042

Table 4: Set Current Voltage Readings

Ameter Reading (A) $\mu$ A	V2 (volt)	R k $\Omega$ (V2/A)
15	0.1	6.667
23	0.2	8.696
37	0.3	8.108
51	0.4	7.843
64	0.5	7.813
83	0.58	6.988
91	0.6	6.593
117	0.7	5.983
129	0.8	6.202
132	0.9	6.818
205	1	4.878
280	1.09	3.893
383	1.19	3.107
492	1.28	2.602
572	1.4	2.448
1765	1.49	0.844
3800	0.4	0.105
3800	0.35	0.092
3500	0.3	0.086
1500	0.25	0.167
500	0.2	0.400
260	0.15	0.577
170	0.1	0.588
55	0.05	0.909

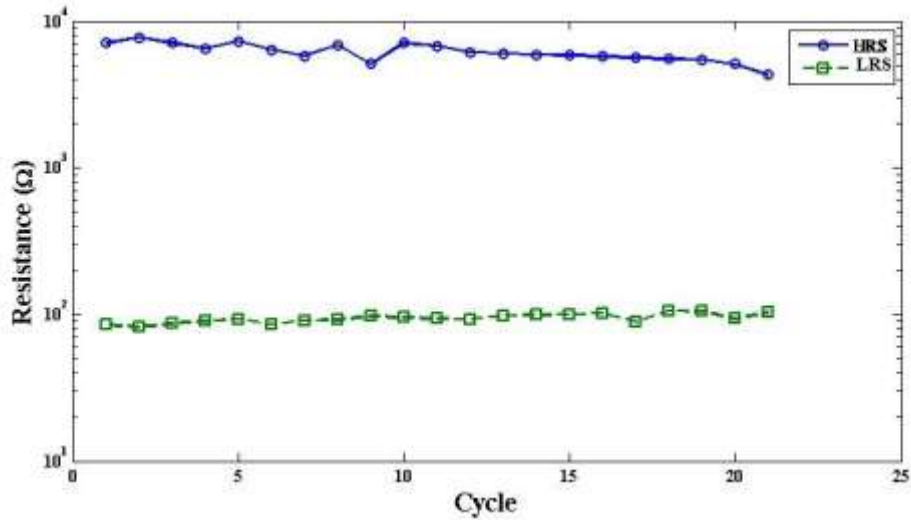


Fig.12: Retention of the RRAM cell for 21 cycle and the resistance was measured after the switching at 0.3 V

Table 5: LRS and HRS readings for 21 cycles

Cycle	RH	RL	Ratio
1	7.086	85	83.365
2	7.73	82	94.268
3	7.1	87	81.609
4	6.5	90	72.222
5	7.3	93	78.495
6	6.4	86	74.419
7	5.8	91	63.736
8	6.9	92	75.000
9	5.1	97	52.577
10	7.12	95	74.947
11	6.8	94	72.340
12	6.13	93	65.914
13	6.03	98	61.531
14	5.94	99	60.000
15	5.84	100	58.400
16	5.75	102	56.373
17	5.65	89	63.483
18	5.55	106	52.358
19	5.46	105	52.000
20	5.1	94	54.255
21	4.3	103	41.748

## Conclusion:

Unipolar switching was investigated using the Al/SnO<sub>2</sub>/Al memory device structure. Optical characteristics of SnO<sub>2</sub> showed a typical properties for Tin Oxide films with average optical band gap of 3.606eV. High resistance was obtained of as deposited device ( $\approx 3.5\text{M}\Omega$ ). The initial resistive switching (IRS) observed at 5.62V (Forming voltage). By applying a voltage range between s(0.68 – 1.5)V, a sudden drop in the leakage current indicating the reset process but a higher current ,than compliance current, was required for a successful reset to HRS (4.3 – 7.7) K $\Omega$ . At (1.13 – 2.5)V a raising in the current is happened so that the set process is achieved with LRS (106 - 82) $\Omega$  . Retention and repeatability showed a good behavior of the device in 21 cycles with small fluctuation in the value of HRS and decreasing after 21 cycles. Note the widely distribution of HRS in comparing with LRS is narrowly distributed. A ratio of HRS to LRS was measured in rang between ( 41 – 94).

## References:-

- [1] Y. Chai, Y. Wu, K. Takei, and H. Chen, “Nanoscale Bipolar and Complementary Resistive Switching Memory Based on Amorphous Carbon”, IEEE Transaction and Electronics Devices, Vol. 58, No.11, PP: 3933-3939, November 2011.
- [2] A. Sawa, “Resistive Switching in Transition Metal Oxides”, Martials today, Vol. 11, No. 6,PP: 28-36, June 2008.
- [3] H.S. P. Wong, S. Kim, B. Lee, M. A. Caldwell, J. L., Y. Wu, R. Jeyasingh, and S. Yu, “Recent Progress of Phase Change Memory (PCM) and Resistive Switching Random Access Memory (RRAM)”, 2011 3rd IEEE International Memory Workshop, pp. 1-5, 2011.
- [4] H.S. P. Wong, “Metal Oxide RRAM”, IEEE, Vol. 100, PP: 1951– 1970, 2012.
- [5] H.S. P. Wong, “Phase Change Memory”, IEEE, Vol. 98, No. 12, pp. 2201–2228, 2010.
- [6] H. Li, and Y. Chen , “An Overview of Non-Volatile Memory Technology and the Implication for Tools and Architectures”, IEEE, Design, Automation & Test in Europe Conference & Exhibition, pp. 731 – 736,2009.
- [7] L. M. Kukreja, A. K. Das, and P. Misra, “Studies on Nonvolatile Resistance Memory Switching in ZnO Thin Films”, Indian Academy of Sciences, Bull. Mater. Sci., Vol. 32, No. 3, pp. 247–252, June 2009.
- [8] W. Chang, Y. Lai, T. Wu, S. Wang, F. Chen, and M. Tsai, “Unipolar Resistive Switching Characteristics of ZnO Thin Films for Nonvolatile Memory Applications”, Applied Physics Letters 92, 022110,2008.
- [9] R. Waser and M. Aono, “Nanoionics-Based Resistive Switching Memories”, Martials today, VOL. 6,PP: 833-840, November 2007.
- [10]K. Nagashima, T. Yanagida, K. Oka, and T. Kawai, “Unipolar Resistive Switching Characteristics of Room Temperature Grown SnO<sub>2</sub> Thin Films”, Applied Physics, Vol 94, PP: 1-3, 2009.
- [11]C. Drake and S. Seal, “Band Gab Energy Modifications Observed in Trivalent In Substituted Nanocryalline SnO<sub>2</sub>”, Applied Physics, Vol 90, PP: 1-3, 2007.
- [12]Abdul Faheem Khan, “Effects of Annealing on Structural, Optical and Electrical Properties of SnO<sub>2</sub>, TiO<sub>2</sub>, Ge and Multi-layer TiO<sub>2</sub>-Ge Thin Films Prepared by Physical Vapor Deposition Techniques”, Dissertation Submitted to Department of Chemical and Materials Engineering, Pakistan Institute of Engineering and Applied Sciences, Islamabad, Pakistan, 2010.

- [13] R. Dhere, H. Moutnho, S. Asher, X. Li, R. Ribelin, and T. Gessert, "Characterization of SnO<sub>2</sub> Films Prepared Using Tin Tetrachloride and Tetra Methyl Tin Precursors", National Renewable Energy Laboratory, CP-520-25733, 1998.
- [14] S. Almeida, B. Aguirre, N. Marques, J. McClure, and D. Zubia, "Resistive Switching of SnO<sub>2</sub> Thin Film on Glass Substrates", *Integrated Ferroelectrics: An International Journal*, Vol: 126:1, PP: 117-124, 2011.
- [15] K. Patel, M. Jani, V. Pathak, and R. Srivastava, "Deposition of CdSe Thin Films By Thermal Evaporation and Their Structural and Optical Properties", *Chalcogenide Letters* Vol.6, No.6, pp: 279-286, 2009.
- [16] Haneafa Yhiea Najem, "Preparation and Study of Optical Electrical and Structural Properties of AL-Doped ZnO Thin Films by Chemical Vapor Deposition (CVD)", Thesis submitted to College of Education, University of Mosul, Mosul, Iraq, 2009.
- [17] E. D. Palik, "Handbook of Optical Constants of Solids", Academic Press, 1998.